Journal of Chromatography A 1718 (2024) 464722

Contents lists available at ScienceDirect

Journal of Chromatography A

journal homepage: www.elsevier.com/locate/chroma

In-line buffer exchange in the coupling of Protein A chromatography with weak cation exchange chromatography for the determination of charge variants of immunoglobulin G derived from chinese hamster ovary cell cultures

Sarah K. Wysor [a], Benjamin F Synoground [b], Sarah W. Harcum [b], R. Kenneth Marcus [a,*]

[a] Department of Chemistry, Biosystems Research Complex, Clemson University, Clemson, SC 29634-0973, USA
[b] Department of Bioengineering, Biosystems Research Complex, Clemson University, Clemson, SC 29634-0973, USA

ARTICLE INFO

Keywords:
Two-dimensional liquid chromatography (2D-LC)
Monoclonal antibodies (mAb)
Protein A (ProA) chromatography
Weak cation exchange (WCX) chromatography
Buffer exchange

ABSTRACT

Immunoglobulin G (IgG) is the most common monoclonal antibody (mAb) grown for therapeutic applications. While IgG is often selectively isolated from cell lines using protein A (ProA) chromatography, this is only a stepping stone for complete characterization. Further classification can be obtained from weak cation exchange chromatography (WCX) to determine IgG charge variant distributions. The charge variants of monoclonal antibodies can influence the stability and efficacy in vivo, and deviations in charge heterogeneity are often cell-specific and sensitive to upstream process variability. Current methods to characterize IgG charge variants are often performed off-line, meaning that the IgG eluate from the ProA separation is collected, diluted to adjust the pH, and then transferred to the WCX separation, adding time, complexity, and potential contamination to the sample analysis process. More recently, reports have appeared to streamline this separation using in-line two-dimensional liquid chromatography (2D-LC). Presented here is a novel, 2D-LC coupling of ProA in the first dimension (^{1}D) and WCX in the second dimension (^{2}D) chromatography. As anticipated, the initial direct column coupling proved to be challenging due to the pH incompatibility between the mobile phases for the two stages. To solve the solvent compatibility issue, a size exclusion column was placed in the switching valve loop of the 2D-LC instrument to act as a means for the on-line solvent exchange. The efficacy of the methodology presented was confirmed through a charge variant determination using the NIST monoclonal antibody standard (NIST mAb), yielding correct acidic, main, and basic variant compositions. The methodology was employed to determine the charge variant profile of IgG from an in-house cultured Chinese hamster ovary (CHO) cell supernatant. It is believed that this methodology can be easily implemented to provide higher-throughput assessment of IgG charge variants for process monitoring and cell line development.

1. Introduction

Therapeutic antibodies have emerged as potent treatments for various diseases due to the ability to target specific antigens [1]. Monoclonal antibodies (mAbs) are particularly versatile therapeutic agents due to the capability to treat cancer, autoimmune diseases, and viral infections [2], while presenting long half-lives and limited side effects [3–6]. Due to popularity, more than 100 therapeutic-based mAbs have been approved for treatments, resulting in a large presence in the biopharmaceutical market, with expectations to reach $300 billion in annual sales by 2025 [7]. The efficacy of mAbs is primarily due to the ability to recognize a single epitope, resulting in high specificity and reduced cross-reactivity [8]. Specifically, the mechanisms of mAb therapeutics include immune modulation, cell signaling, metastasis, apoptosis, and effector function modalities [9]. The scope of application of mAbs continues towards a greater variety of diseases, increasing the number of therapeutic antibody products. With this growth, there is a drive to produce antibodies more efficiently and cost-effectively, while maintaining consistency and shelf-life.

One of the primary attributes in mAb production is the micro-heterogeneity within and between lots. While microheterogeneity in mAb production is expected, any production changes can also result in

* Corresponding author.
E-mail address: marcusr@clemson.edu (R.K. Marcus).

https://doi.org/10.1016/j.chroma.2024.464722
Received 5 January 2024; Received in revised form 5 February 2024; Accepted 7 February 2024
Available online 10 February 2024

additional mAb modifications through enzymatic processes, spontaneous degradation/modifications, and chemical degradations [4]. These modifications can ultimately affect the stability, potency, and bioactivity of the mAb. As heterogeneity can negatively affect the pharmacokinetics of therapeutic mAbs, and lot-to-lot variability is known to occur [10,11], there is a great need for more thorough mAb characterization and quality control. The charge variant state of the product mAbs is considered a primary quality attribute (QA) of the process due to its impact on bioactivity [12,13], necessitating regulation by authorities such as the US Food and Drug Administration [14,15]. Charge variants of mAbs are commonly determined through liquid chromatography (LC) [16], mass spectrometry (MS) [17], or capillary electrophoresis (CE) [18]. Ion exchange chromatography (IEX) [19] is perhaps the most widely applied LC methodology due to the robustness, resolving power, and non-denaturing conditions of the separation [20]. Both anion [21] and cation [4,12,22] exchange chromatography have been used for charge variant determination, with the cation variant being more prevalent due to the basic isoelectric points (pIs) exhibited by mAbs. Cation exchange separations are commonly employed for mAbs, involving salt [12,13,23] or pH [22,24,25] gradients have proven capable of separating mAbs differing by a single charge unit [3]. Increasing the salt concentration or pH of the mobile phase causes the molecules with the weakest ionic interaction to elute first, followed by the strongest [19]. In the case of IgG, the acidic species will have the weakest ionic interaction, while the basic species will have the strongest ionic interaction. Both strong cation exchange chromatography (SCX) using sulphonic acid ligands [26–28] and weak cation exchange chromatography (WCX) using carboxylic acid ligands [29–31] are employed for charge variant separations of mAbs.

Charge variant analysis is often a complex multi-step process [32–35]. Before determining the charge variants, the mAbs, specifically immunoglobulin G (IgG), must be isolated from the complex cell culture matrix of host cell proteins, cell debris, and various other waste components inherent to the bioprocess. Protein A (ProA) chromatography is the most common and gold standard purification modality for IgG, where the antibody exhibits a specific binding affinity for the protein A stationary phase ligand [36]. As such, ProA isolation is routinely performed as the initial chromatographic step in the process. ProA separations rely on the neutral pH binding buffer for IgG capture, followed by a low pH (~2.5) elution buffer to disrupt the hydrogen bonds between IgG and protein A to effect elution [37,38]. A complicating factor here is that the low pH elution can result in protein aggregation [39,40]. As such, the recovered target eluate must be neutralized prior to any further characterization, e.g., charge variant analysis. This adjustment is most often completed offline, as such, affecting further on-line chromatographic modalities in a two-dimensional liquid chromatography (2D-LC) format following ProA is very challenging.

Here we present a novel coupling of ProA and WCX using 2D-LC for the high throughput isolation and charge variant determination of IgG. While researchers have coupled ProA with ion exchange chromatography (IEX) offline, recently 2D-LC experiments have been introduced using heartcut methods and specialty valves [41–43]. However, additional instrumentation is required, or only a fraction of the IgG eluate is transferred to the ^{2}D during heartcut methods, meaning the IEX separation is not representative of the entire population. Additionally, the eluate from the ProA separation is a high salt/conductivity solution and low pH which is not ideal for binding conditions. This results in decreased retention and the tendency of IgG to fold onto itself, hiding potential binding sites [44,45]. Moreover, IEX has been coupled with size exclusion chromatography (SEC) or reversed-phase chromatography (i.e., IEX x SEC and IEX x RP) to determine charge variants of mAbs [31,46–48], with the primary isolation of IgG being a discrete unit operation. To address the solvent incompatibility and circumvent the off-line sample manipulation, an SEC column has been implemented here into the switch valve loop of the 2D-LC workflow (between ProA and WCX) to achieve a stationary phase assisted solvent exchange. This placement also acted as a transfer modality to ensure the entire fraction of IgG from ProA is transferred to the WCX column in ^{2}D. The SEC column was added purely for solvent exchange and not to enhance chromatographic performance, but it was not initially successful for the eluate transfer between the ProA and WCX methods. As previously mentioned, the low pH of the ProA elution solvent can lead to IgG aggregation, compromising retention on the WCX column. Therefore, arginine was added to the primary, acidic ProA elution solvent, as it has been shown to prevent aggregation and improve recovery [40,49]. Together, the solvent exchange and the SEC column were effective in the transfer between the ProA and WCX columns, where the absorbance peak area response confirmed unit recoveries in the transfer process. The quantitative recoveries and the accuracy and run-to-run repeatability of the charge variant determinations through the overall 2D-LC coupled method were verified using the National Institutes of Standards and Technology Monoclonal Antibody Reference Material 8671 (NIST mAb). Following the method verification, the coupling was tested using the complex supernatant of in-house cultured Chinese hamster ovary (CHO) cells, yielding high levels of recovery and run-to-run repeatability. It is believed that the 2D-LC method employing an in-line SEC column to effect buffer exchange will provide improved performance and higher throughput than currently realized in most IgG charge variant determinations.

2. Materials and methods

2.1. Chemicals and columns

Sodium phosphate, monobasic, monohydrate (EMD Millipore, Merck, Germany), sodium phosphate, di-basic, heptahydrate (EMD Millipore, Merck), citric acid (BDH, Dubai, United Arab Emirates), sodium chloride (Alfa Aesar, Ward Hill, MA, USA) and arginine hydrochloric acid (TCI, Tokyo, Japan) were used for ProA and WCX separations. Deionized water (DI-H_2O) for solvent preparation was obtained from an Elga PURELAB flex water purification system, (18.2 MΩ-cm, Veolia Water Technologies, High Wycombe, England). Monoclonal Antibody Reference Material 8671 (NIST, Gaithersburg, MD, USA) was used as a standard for ProA and WCX separations, with charge variants certified as 16.01 – 17.11 %, 72.99 – 74.65 %, and 8.99 – 10.25 % for acidic, main, and basic, respectively. All columns for the separations were from Agilent Technologies (Santa Clara, USA) and include: bio-monolith recombinant protein A, 4.95 mm x 5.2 mm, bio SEC-5, 5 µm, 500 Å, 4.6 mm x 300 mm, and bio WCX, NP5, 4.6 × 250 mm PEEK. Supernatant from an IgG_1-producing Chinese hamster ovary (CHO) cell line, CHOZN®GS23 (MilliporeSigma, Burlington, MA), was cultured in the Harcum laboratory (Department of Bioengineering, Clemson University). Both the cell line and AMBIC 1.1 basal media and feeds used for culturing were shared by MilliporeSigma as part of an Advanced Mammalian Biomanufacturing Innovation Center (AMBIC)-funded project [50].

2.2. Instrumentation

All chromatographic separations were performed using an Agilent 2D HPLC (Agilent, Technologies, Santa Clara, CA), which includes a 1260 binary pump, 1260 degasser, 1260 Multisampler, 1100 multiple wavelength detector, 1290 valve drive, 1290 ultra-high performance liquid chromatography (UHPLC) high-speed pump, and 1290 variable wavelength detector. 2D-LC instrumentation was operated using OpenLab ChemStation Edition Software. Injection volumes for separations varied between 100 – 500 µL.

2.3. Methods

2.3.1. Protein A chromatography

Mobile phases for the ProA separation were 20 mM sodium

phosphate, pH 7 (MP A), and 250 mM arginine hydrochloride, pH 2.5 (MP B). A step gradient was used for the separation, with a two-minute column equilibration with 100 % MP A followed by a step to 100 % MP B for two minutes. Arginine was added to the ProA citric acid elution buffer to minimize the aggregation of IgG at the low pH required for elution. A flow rate of 1.0 mL min^{-1} and absorbance detection 280 nm was used for all ProA separations. Mobile phases were pH adjusted as needed using suitable aliquouts of NaOH and HCl.

2.3.2. *Weak cation exchange chromatography*

For one-dimensional WCX separations, 20 mM sodium phosphate, pH 7 (MP C), and MP C + 0.5 M sodium chloride (MP D) were used. A linear gradient resulting in 0.16 %B min^{-1} was used to resolve the charge variants of IgG, with the gradient program as follows: 0–4 min, 0 % D; step to 5 % D at 4 min; 4 – 34 min, from 5 – 10 % D; 34 – 36 min, 100 % D, 36 – 40 min, 0 % D. Again, a flow rate of 1.0 mL min^{-1} and absorbance detection at 280 nm was employed. The charge variants were quantified using the peak area of each variant as described in [51]. One-dimensional separations were performed prior to the 2D-LC coupling method to confirm each separation coupling individually.

2.3.3. *2D-LC coupling method*

The complete column coupling and valving can be found in Fig. 1, representing each of the respective steps in the separation workflow, where the ProA column is in ^{1}D, the WCX column is in ^{2}D, and the SEC column was placed in the loop of the switch valve. As the SEC column placement is the innovation of the charge variant method, the coupling/placement of the SEC column in the switch valve is detailed here. Additionally, the solvent parameters for each step of the separation can be found in Table 1. Initially, no SEC column was placed in the loop, with a standard transfer directly from the ProA phase at low pH, filling the ^{2}D injection loop, and followed by elution to the WCX column in the neutral-pH buffer. A 400 µL sample was injected onto the ProA column. This method yielded very poor ^{2}D retention and unsuccessful charge state differentiation. The addition of the SEC column, effectively as the injection loop, provides an environment where the antibodies can be "parked" and eluted from the column with the WCX buffer, effecting a mode of solvent exchange. For the first step of the separation, the 400 µL sample is injected onto the ProA column at 1.0 mL min^{-1} (Fig. 1a.), where IgG is captured, and all other matrix species flow through unretained into the waste (0 – 2 min). Subsequently, the ProA column is switched to be in-line with the SEC column (Fig. 1b.), still at a flow rate of 1.0 mL min^{-1}, where the captured IgG is eluted using MP B (citric acid/arginine) onto the SEC column (2 – 4 min). After the IgG is eluted from the ProA column, the solvent is changed back to MP A, and the IgG is passed through the SEC column (4 – 10 min). Once the IgG fraction has traveled approximately three-quarters of the way through the SEC column, (determined based on IgG elution time on the SEC column) the valve is switched to put the SEC flow in-line with the WCX column (Fig. 1c.). With the switch, the flow is reversed as the ^{2}D pump now flows MP C through the SEC column and to the WCX at a lower flow rate of 0.4 mL min^{-1} (10 – 40 min) due to the low backpressure limit of the SEC column. Once the IgG plug has been completely transferred to the WCX column, the SEC column is switched out of line (Fig. 1d) and the ^{2}D flow rate is gradually increased from 0.4 mL min^{-1} to 1.0 mL min^{-1} (40 – 50 min) and equilibrated with MP C (50 – 55 min). Finally, the linear gradient for the charge variants elution starts and goes from 5 % - 10 % MP D (55 – 85 min), followed by a 100 % MP D wash (85 – 87 min), and then back to 100 % MP C for re-equilibration from (87 – 90 min).

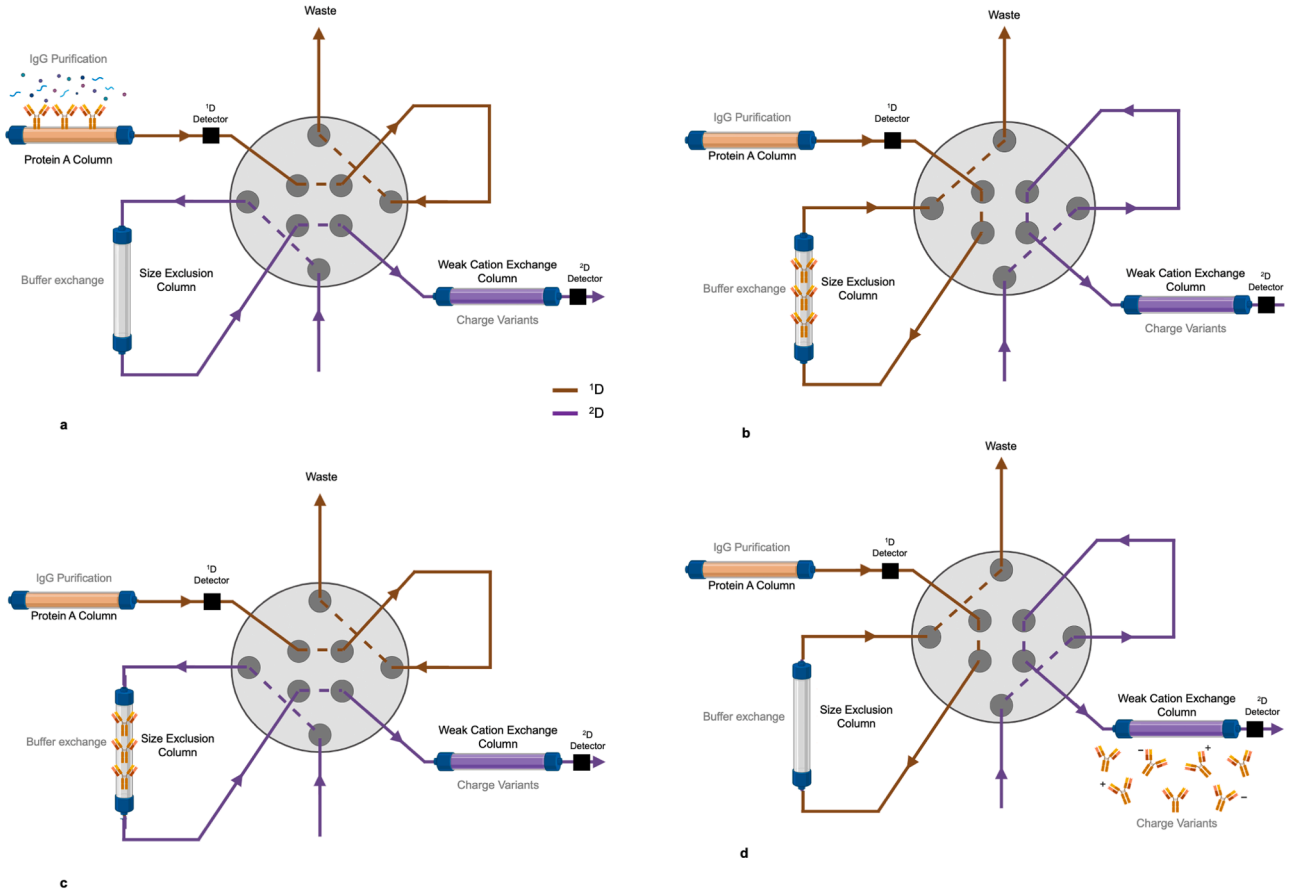

Fig. 1. Diagram of 2D-LC column coupling, displaying a) the capture of IgG on the ProA column in ^{1}D, b) the transfer of the IgG plug to the SEC column in-line with the ProA column, c) transfer from the SEC column to the WCX column for charge variant determinations, and d) elution from the WCX column.

Table 1
Switch valve orientation and solvent programming for 2DLC- ProA x SEC x WCX IgG charge variant determinations.

Orientation	Parameter	1D	2D
Sample Injection/ Fig. 1a	Columns in-line	ProA x detector-1 x waste	
	Flow Rate (mL min^{-1})	1.0	0.4
	Gradient	100 % MP A (0 – 2 min)	100 % MP C (0 – 2 min)
IgG elution to SEC/Fig. 1b	Columns in-line	ProA x SEC	
	Flow Rate (mL min^{-1})	1.0	0.4
	Gradient	100% MP B (2 – 4 min); 4 – 10 min MP A	100 % MP C (2 – 10 min)
Transfer of IgG to WCX/ Fig. 1c	Columns in-line	SEC x WCX	
	Flow Rate (mL min^{-1})	1.0	0.4
	Gradient	100 % MP A (10 – 40 min)	100 % MP C (10 – 40 min)
Elution of IgG from WCX/ Fig. 1d	Columns in-line	WCX x detecto-2 x waste	
	Flow Rate (mL min^{-1})	1.0	0.4 – 1.0 (40 – 50 min)
	Gradient	100 % MP A (40 – 90 min)	40 – 55 min MP C; 5 - 10 % MP D (55 – 85 min); 100 % MP D (85 – 87 min); 100 % MP C (87 – 90 min)

3. Results and discussion

3.1. ProA separation

Prior to coupling the two chromatographic modalities, separations were performed in a standalone (1D) format to verify the individual operations. The standard ProA separation was tested by injecting a 100 µL of 0.28 mg mL^{-1} CHO IgG supernatant. The affinity-based separation relies on the modulation of the pH of the loading and elution solvents for the capture and elution of IgG. For IgG capture, a neutral pH of 7 is used, while for the elution, an acidic pH of 2.5 was used. Studies have found that the acidic pH of the eluent increases the amount of aggregation within the IgG, when a typical mobile phase of 0.1 M citric acid at a pH of 2.9 was used [40], with approximately 40 % of the IgG eluate determined to be aggregated based on subsequent SEC separations. Additionally, when the eluate is transferred off-line to WCX, the aggregate was still present, negatively affecting the charge variant separation. The reduction of antibody aggregation through the addition of arginine to the eluent has been proven successful in multiple studies [39,40,49]. As post-ProA aggregation leads to challenges for any further chromatographic processing of antibodies, arginine was incorporated in the ProA eluent. Additionally, efforts to increase the pH were attempted to lessen the effects of the pH range between the ProA (~2.5) and WCX separation (~7). The recovery of IgG using 100 mM citric acid and 150 mM arginine at pH 2.5, 3.5, 4.5 as elution solvents was evaluated. A typical chromatogram of the protein A processing is shown in Fig. 2. The target antibody was successfully recovered at ~99 % when using the NIST mAb standard for elution at both pH 2.5 and 3.5 (citric acid and arginine); however, at pH 4.5 the recovery dropped to negligible levels. With the quantitative recovery of IgG using arginine addition at a pH 3.5 confirmed, the protocol was used in all ProA separations moving forward.

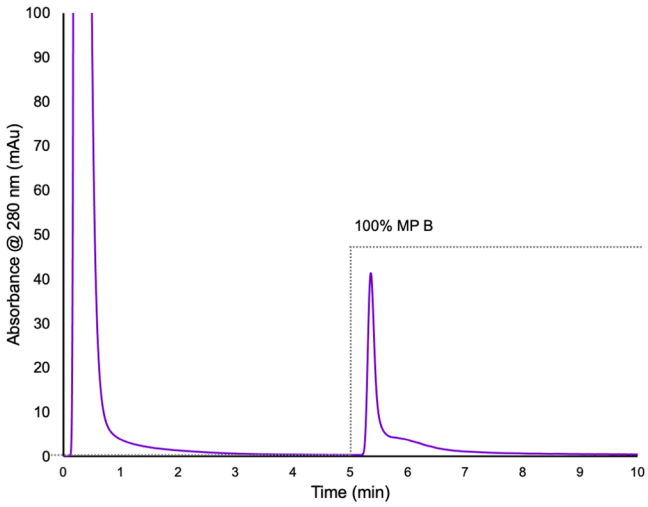

Fig. 2. ProA isolation of IgG, with MP A 20 mM sodium phosphate for binding, pH 7 and MP B 100 mM arginine HCl, pH 2.5 for elution. Absorbance measured @ 280 nm. Flow rate of 1.0 mL min^{-1}. A 100 µL injection of 0.28 mg mL^{-1} CHO IgG supernatant.

3.2. WCX separation

For WCX separations, a salt gradient was used for the isolation of IgG charge variants based on differing charged isoforms [52]. To verify the effectiveness of the method, the charge variant-defined NIST mAb standard was used. For the isolation of the NIST mAb charge variants a linear gradient of 0.16 % MP B min^{-1} was successful at obtaining the correct charge state distribution. For the NIST standard, the charge variant ranges are 16.01 – 17.11 %, 72.99 – 74.65 %, and 8.99 – 10.25 % respectively for the acidic, main, and basic fraction. Fig. 3 presents the average WCX chromatogram for triplicate NIST mAb injections, with the species determined as: acidic as 17.17 % (1.19 % relative standard deviation (RSD)), main as 73.53 % (0.39 % RSD), and basic as 9.30 % (1.20 % RSD). Each of the species was within the defined NIST ranges, except for the acidic species, though having a charge variant percentage within 0.06 % of the certified range. The run-to-run repeatability of the separations over three runs proved to be excellent, with all %RSD values falling under 2 % RSD. Based on the excellent agreement between the

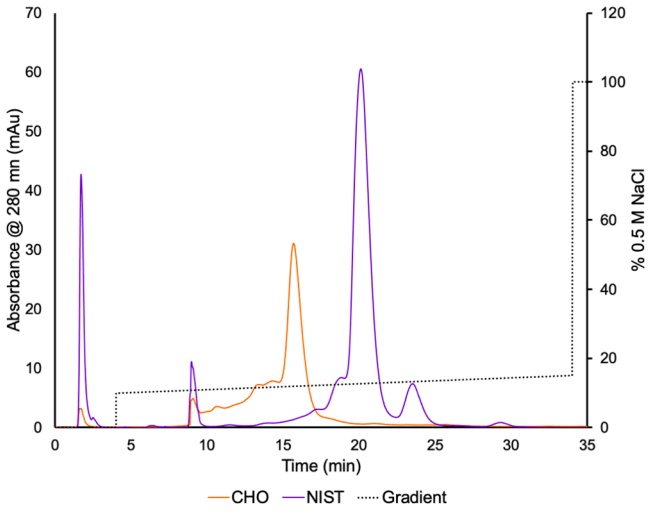

Fig. 3. WCX separation of charge variants of NISTmAb IgG (purple) and CHOZN®GS23-derived IgG (orange) IgG at a flow rate of 1.0 mL min^{-1}. Absorbance measured @ 280 nm. Injection volume of 100 µL for 1.0 mg mL^{-1} NISTmAb and 0.50 mg mL^{-1} CHO IgG supernatant.

certified values and equally high level of run-to-run repeatability, the developed method was considered successful, and the same gradient (0.16 % MP B min^{-1}) was used for all WCX separations moving forward.

With the WCX separation verified, pre-isolated IgG from the in-house CHO cell supernatant was processed through the method as a preliminary determination of the charge variants. That CHO IgG charge variant isolation is presented in Fig. 3 along with the NIST mAb separation. Due to the differing isoelectric points (pIs) of the samples (CHOZN IgG pI: 8.3 – 8.7 versus NIST IgG pI: 9.0 – 9.5), the CHO-derived variants elute sooner (i.e., lower salt concentration) than the NIST mAbs, but were well resolved using the shallow gradient. Again, triplicate runs were performed with the average charge variants as follows: acidic as 38.73 % (0.22 % RSD), main as 53.70 % (0.63 % RSD), and 7.57 % (3.39 % RSD). For the CHO IgG, the acidic variant is predominant, while very little is observed for the basic variant. Increases in the acidic species' fraction have been linked to longer incubation times [53], likely due to sialic acid content or deamidation of asparagine residues [54,55]. Again, excellent run-to-run repeatability was observed, with each showing variability of better than 4 % RSD.

3.3. 2D-LC via ProA x SEC x WCX

The determination of IgG titers and charge variant distributions are essential parts of the screening of IgG produced from cell lines for pharmaceuticals. For the overall coupling of the 2D-LC separation, the ProA column was initially placed in the ^{1}D, and the WCX column in the ^{2}D, using the standard switch valve loop between the two in a heart-cutting fashion. This direct transfer from ProA to WCX proved to be ineffective, as the IgG was transferred from the ProA separation in the low pH (~2.5) citric acid/arginine solvent to the WCX column. With this transfer, the solvent mismatch was too great, as the pH of the WCX separation was ~7 in 0.5 M NaCl and the conductivity of the ProA eluate was too high for efficient IgG retention on the WCX phase, resulting in significant sample loss.

To solve the solvent mismatch, an SEC column was placed in the switch valve loop, shown in Fig. 1 as a stationary phase to facilitate the solvent exchange. The entire method, with the incorporation of the SEC column, is shown overlaid on the chromatogram in Fig. 4 for triplicate injections of 400 μL of 0.67 mg mL^{-1} CHO IgG supernatant. The chromatogram in Fig 4. is from the ^{2}D detector, therefore only the WCX elution is shown. The ^{1}D detector was used to monitor the ProA separation, as shown in Fig. 1. The first portion in blue represents the ProA separation, where the sample is injected, and then only the eluted IgG plug is transferred to the SEC column (Fig. 1b and Fig. 4). The combination of the ProA and the SEC columns do not significantly increase the overall backpressure, so the columns can run in-line at the working flow rate of 1.0 mL min^{-1}. At 1.0 mL min^{-1}, the time it takes for the IgG plug to travel completely through the SEC column was determined (based on the elution time of IgG with the SEC column) to be ~10 min. Therefore, the IgG plug from the ProA elution was allowed to flow through the SEC column for 8 min (~75 % of the breakthrough of the column), as displayed in yellow, to fully capture the entire IgG plug and ensure no sample was lost. After the transfer to the SEC column, the line is switched where the SEC column is placed in-line with the flow to the WCX column (Fig. 1c), shown in orange in Fig. 4. Due to the maximum backpressure limit of the SEC column, and the high operating backpressure from the WCX column, the flow rate is reduced to 0.4 mL min^{-1}. The peak at ~27 min reflects the solvent exchange from the ProA eluent passing through the WCX column. Once the IgG plug is transferred to the WCX column (t=~40 min), the switch valve orientation is changed so that the SEC column is no longer in line with the WCX column, and the flow rate is brought back up to 1.0 mL min^{-1}. Finally, the WCX separation is represented by the green section in Fig. 4.

Having developed the integrated method, the efficacy of the complete 2D-LC method (ProA x SEC x WCX) was demonstrated using the NISTmAb standard, shown in Fig. 5 with on the WCX portion of the chromatogram displayed. With the coupled method, the charge variant determinations were all within defined ranges, with acidic as 16.2 % (0.86 % RSD), main as 73.9 % (0.25 % RSD), and basic as 9.86 % (2.95 % RSD). As expected, there is slight peak broadening due to the length of the separation; however, the charge variants are still isolated within the provided ranges of the standard, along with excellent run-to-run repeatability. Additionally, the percentage recovery of the 3-column transfer method was determined to be 99.4 %, reflecting a near-unit efficiency for the transfer method. Following the confirmation of the NIST mAb standard, the charge variants of a different in-house CHO supernatant sample were determined. The chromatogram for the CHO isolation is also displayed in Fig. 5. Again, there is a difference in the retention time due to the different pIs of the IgG analytes. The WCX separation of the IgG from CHO supernatant, displays 6 discernible peaks among the acidic species. Different from what was observed in Fig. 3, a few basic species are observed, with three distinct peaks found in the basic region. For the charge variant isolation, the acidic, main,

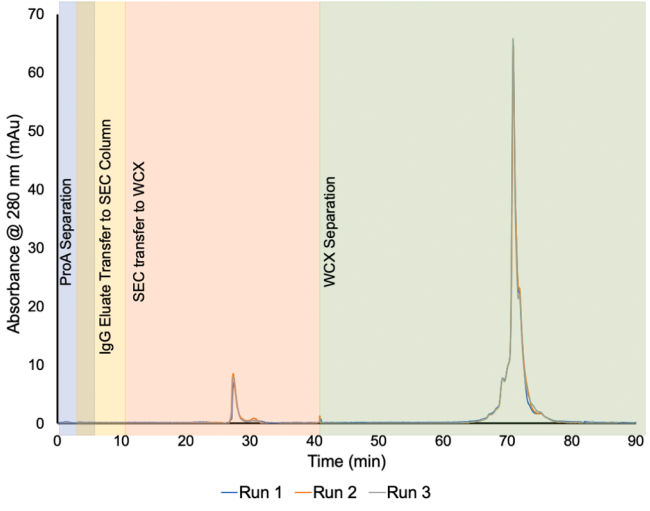

Fig. 4. ^{2}D absorbance response for 2D-LC ProA x SEC x WCX separation, with labeled steps: ProA separation (blue), transfer from ProA to SEC column (yellow), transfer from SEC to WCX column (orange), WCX separation (green). Injection volume of 400 μL of 0.67 mg mL^{-1} CHO IgG supernatant. Absorbance measured @ 280 nm.

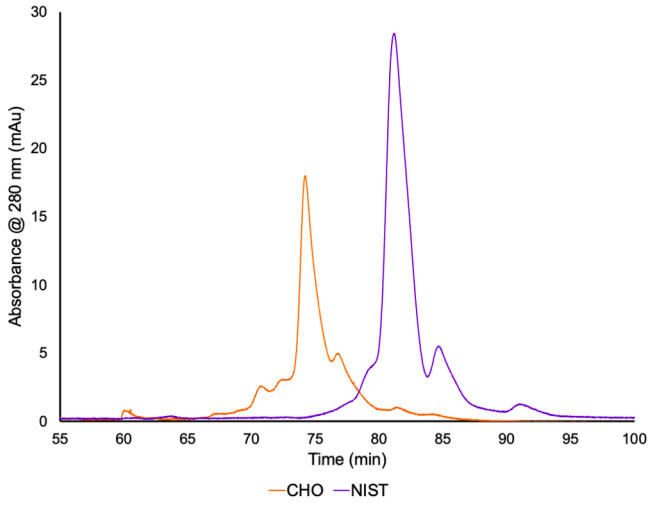

Fig. 5. ^{2}D WCX separation of NIST IgG (purple) and CHOZN®GS23-derived IgG (orange). Absorbance measured @ 280 nm. Gradient 0.16 %B min^{-1} and 1.0 mL min^{-1} flow rate. 400 μL of a 0.5 mg mL^{-1} NISTmAb solution and 0.43 mg mL^{-1} of CHO IgG supernatant.

and basic were determined to be 30.9 % (1.61 % RSD), 44.9 % (0.38 % RSD), and 24.1 % (1.73 % RSD), respectively. The charge variants were not expected to be the same as before as the samples were taken from different CHO supernatants. The confirmation of the charge variant determinations was confirmed using the NIST mAb and provides certainty in using this workflow to accurately reflect the charge variant state of different process samples.

3.4. Evaluation of process recoveries

The linearity of the recoveries of the transfer from ^{1}D ProA to the ^{2}D WCX, with the placement of the SEC in the switch valve, was evaluated by loading various volumes of supernatant. CHO supernatant volumes ranging from 100 µL to 500 µL at a concentration of 0.5 mg mL^{-1} IgG (50 – 250 µg on-column) were injected. As a first consideration, the linearity of the IgG absorbance response from the ProA separation was evaluated across injection volumes of 100 – 500 µL. A linear response was observed for the ProA elution across the volume range, with a linear regression of $y = 0.3075x + 12.71$, $R^2 = 0.9930$. As the ProA elution was unaffected by the loading volume and produced a linear response, the percentage of each variant from the ^{2}D WCX separation was determined for each injection volume. The ^{2}D WCX chromatograms across each injection are shown in Fig. 6. To determine the linearity of the transfer, the peak areas of the acidic, main, and basic variants were plotted versus the volume of supernatant loaded. For each, the peak area was determined through integration of the chromatogram, by identifying the three variants of the separation. The variants consisted of the acidic, or everything to the left of the main peak (~50 – 74 min), the main peak in the center (~74 – 77 min), and finally the basic peak, or everything to the right of the main peak (~77 - 100). A linear response was observed across each of the charge variants, with each response function exhibiting an R^2 of greater than 0.95. The linear regressions for acidic, main, and basic were $y = 0.1247x - 6.8756$ ($R^2 = 0.9643$), $y = 0.1038x - 6.6380$ ($R^2 = 0.9920$), and $y = 0.0701x - 4.4125$ ($R^2 = 0.9547$). The charge variants across each volume loaded were ~42 % (4.65 % RSD), ~35 % (3.99 % RSD), and ~23 % (4.14 % RSD) for acidic, main, and basic, respectively. While all of the precision values are better than 5 % RSD, the variabilities were slightly higher for the lowest injection volume, reflecting the low absorbance responses. Indeed, if the data for the 100 µL injections is removed, the precision is significantly improved with acidic as ~41 % (0.73 % RSD), main as ~35 % (2.04 % RSD), and basic as 23.3 % (2.91 % RSD). The excellent agreement of charge variants across various volumes, along with the linear response in peak areas, proves that the ^{2}D WCX separation can serve as an additional mode of quantification (along with ^{1}D ProA), displaying excellent reveries throughout the transfer.

4. Conclusions

Overall, this 2D-LC coupling methodology proves to be a successful separation and determination of charge variants of IgG, which can be easily implemented to model the change of IgG charge profiles over a cell growth cycle. The cell culture supernatant sample only needs to be passed through a standard 0.2 µm syringe filter before the separation. The methodology provides a fully automated separation through the novel placement of the SEC column in the 2D-LC switch valve. Using this coupling, the run-to-run repeatability was proved to be excellent as the percent RSD was under 4 % for all separations. Additionally, due to the linearity across injection volumes, the WCX isolation can serve as a quantitative measurement of IgG charge variants. Additionally, this coupling shows how an SEC column can be implemented as a mode of solvent exchange in additional coupling strategies. Further efforts will look at implementing capillary-channeled polymer (C—CP) fiber ProA and WCX stationary phases into this methodology to reduce the separation time and concentration requirements of the method [56–59], with the anticipation of improving the overall process throughput and reducing the component costs.

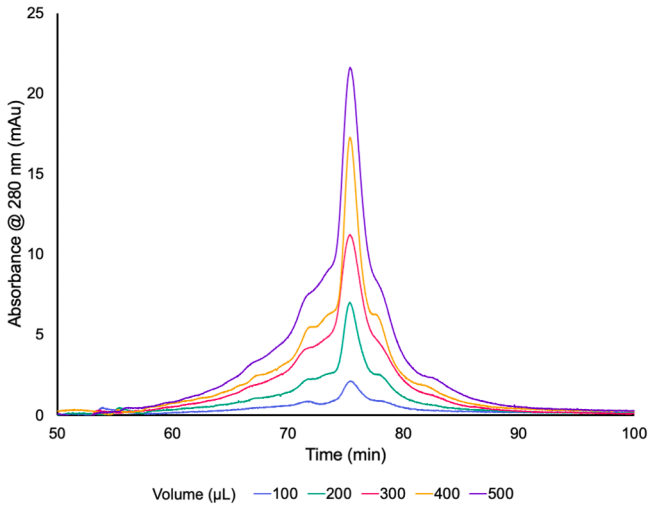

Fig. 6. ^{2}D WCX separation of CHO IgG for injection volumes from 100 – 500 µL of 0.5 mg mL^{-1} CHO IgG supernatant. Gradient 0.16 %B min^{-1} and 1.0 mL min^{-1} flow rate.

CRediT authorship contribution statement

Sarah K. Wysor: Methodology, Data curation, Visualization, Writing – original draft. **Benjamin F Synoground:** Methodology. **Sarah W. Harcum:** Supervision, Writing – review & editing. **R. Kenneth Marcus:** Conceptualization, Supervision, Writing – review & editing.

Declaration of competing interest

The authors declare the following financial interests/personal relationships which may be considered as potential competing interests: R. Kenneth Marcus reports financial support was provided by National Science Foundation. Sarah W. Harcum reports financial support was provided by National Science Foundation. If there are other authors, they declare that they have no known competing financial interests or personal relationships that could have appeared to influence the work reported in this paper.

Data availability

Data will be made available on request.

Acknowledgements

Funding from the National Science Foundation under grant no. CHE-2107882 to RKM and from the National Science Foundation under grant no. EEC-2100442 and through the membership fees of the Advanced Mammalian Biomanufacturing Innovation Center (AMBIC) to SWH, is gratefully acknowledged.

References

[1] P. Chames, M. Van Regenmortel, E. Weiss, D. Baty, Therapeutic antibodies: successes, limitations and hopes for the future, Br. J. Pharmacol. 157 (2) (2009) 220–233, https://doi.org/10.1111/j.1476-5381.2009.00190.x.
[2] R.M. Lu, Y.C. Hwang, I.J. Liu, C.C. Lee, H.Z. Tsai, H.J. Li, H.C. Wu, Development of therapeutic antibodies for the treatment of diseases, J. Biomed. Sci. 27 (1) (2020) 1, https://doi.org/10.1186/s12929-019-0592-z.
[3] A. Farjami, M. Siahi-Shadbad, P. Akbarzadehlaleh, O. Molavi, Development and validation of salt gradient CEX chromatography method for charge variants separation and quantitative analysis of the IgG mAb-cetuximab, J. Chromatogr. A 81 (12) (2018) 1649–1660, https://doi.org/10.1007/s10337-018-3627-9.
[4] L.A. Khawli, S. Goswami, R. Hutchinson, Z.W. Kwong, J. Yang, X. Wang, Z. Yao, A. Sreedhara, T. Cano, D. Tesar, I. Nijem, D.E. Allison, P.Y. Wong, Y.H. Kao, C. Quan, A. Joshi, R.J. Harris, P. Motchnik, Charge variants in IgG1: isolation,

characterization, in vitro binding properties and pharmacokinetics in rats, MAbs 2 (6) (2010) 613–624, https://doi.org/10.4161/mabs.2.6.13333.
[5] R.J. Ober, C.G. Radu, V. Ghetie, E.S. Ward, Differences in promiscuity for antibody–FcRn interactions across species: implications for therapeutic antibodies, Int. Immunol. 13 (12) (2001) 1551–1559, https://doi.org/10.1093/intimm/13.12.1551.
[6] P. Carter, Improving the efficacy of antibody-based cancer therapies, Nat. Rev. Cancer 1 (2) (2001) 118–129, https://doi.org/10.1038/35101072.
[7] A.C. Szkodny, K.H. Lee, Biopharmaceutical manufacturing: historical perspectives and future directions, Annu. Rev. Chem. Biomol. Eng. 13 (1) (2022) 141–165, https://doi.org/10.1146/annurev-chembioeng-092220-125832.
[8] J.D. Berry, Rational monoclonal antibody development to emerging pathogens, biothreat agents and agents of foreign animal disease: the antigen scale, Vet. J. 170 (2) (2005) 193–211, https://doi.org/10.1016/j.tvjl.2004.04.021.
[9] D. Zahavi, L. Weiner, Monoclonal antibodies in cancer therapy, Antibodies (Basel) 9 (3) (2020), https://doi.org/10.3390/antib9030034.
[10] S. Sundaram, A. Matathia, J. Qian, J. Zhang, M.C. Hsieh, T. Liu, R. Crowley, B. Parekh, Q. Zhou, An innovative approach for the characterization of the isoforms of a monoclonal antibody product, MAbs 3 (6) (2011) 505–512, https://doi.org/10.4161/mabs.3.6.18090.
[11] D. Ayoub, W. Jabs, A. Resemann, W. Evers, C. Evans, L. Main, C. Baessmann, E. Wagner-Rousset, D. Suckau, A. Beck, Correct primary structure assessment and extensive glyco-profiling of cetuximab by a combination of intact, middle-up, middle-down and bottom-up ESI and MALDI mass spectrometry techniques, MAbs 5 (5) (2013) 699–710, https://doi.org/10.4161/mabs.25423.
[12] S. Fekete, A. Beck, J. Fekete, D. Guillarme, Method development for the separation of monoclonal antibody charge variants in cation exchange chromatography, Part I: salt gradient approach, J. Pharm. Biomed. Anal. 102 (2015) 33–44, https://doi.org/10.1016/j.jpba.2014.08.035.
[13] S. Fekete, A. Beck, J. Fekete, D. Guillarme, Method development for the separation of monoclonal antibody charge variants in cation exchange chromatography, Part II: pH gradient approach, J. Pharm. Biomed. Anal. 102 (2015) 282–289, https://doi.org/10.1016/j.jpba.2014.09.032.
[14] S. Flatman, I. Alam, J. Gerard, N. Mussa, Process analytics for purification of monoclonal antibodies, J. Chromatogr. B 848 (1) (2007) 79–87, https://doi.org/10.1016/j.jchromb.2006.11.018.
[15] H. Liu, G. Gaza-Bulseco, D. Faldu, C. Chumsae, J. Sun, Heterogeneity of monoclonal antibodies, J. Pharm. Sci. 97 (7) (2008) 2426–2447, https://doi.org/10.1002/jps.21180.
[16] R.L. Fahrner, H.L. Knudsen, C.D. Basey, W. Galan, D. Feuerhelm, M. Vanderlaan, G. S. Blank, Industrial purification of pharmaceutical antibodies: development, operation, and validation of chromatography processes, Biotechnol. Genet. Eng. Rev. 18 (1) (2001) 301–327, https://doi.org/10.1080/02648725.2001.10648017.
[17] A. Beck, S. Sanglier-Cianférani, A. Van Dorsselaer, Biosimilar, biobetter, and next generation antibody characterization by mass spectrometry, J. Anal. Chem. 84 (11) (2012) 4637–4646, https://doi.org/10.1021/ac3002885.
[18] C.E. Espinosa-de la Garza, R.D. Salazar-Flores, N.O. Pérez, L.F. Flores-Ortiz, E. Medina-Rivero, Capillary electrophoresis separation of monoclonal antibody isoforms using a neutral capillary, J. Vis. Exp. 119 (2017), https://doi.org/10.3791/55082.
[19] S. Fekete, A. Beck, J.L. Veuthey, D. Guillarme, Ion-exchange chromatography for the characterization of biopharmaceuticals, J. Pharm. Biomed. Anal. 113 (2015) 43–55, https://doi.org/10.1016/j.jpba.2015.02.037.
[20] D. Farnan, G.T. Moreno, Multiproduct high-resolution monoclonal antibody charge variant separations by ph gradient ion-exchange chromatography, J. Anal. Chem. 81 (21) (2009) 8846–8857, https://doi.org/10.1021/ac901408j.
[21] G. Teshima, M.X. Li, R. Danishmand, C. Obi, R. To, C. Huang, J. Kung, V. Lahidji, J. Freeberg, L. Thorner, M. Tomic, Separation of oxidized variants of a monoclonal antibody by anion-exchange, J. Chromatogr. A 1218 (15) (2011) 2091–2097, https://doi.org/10.1016/j.chroma.2010.10.107.
[22] M. Talebi, A. Nordborg, A. Gaspar, N.A. Lacher, Q. Wang, X.Z. He, P.R. Haddad, E. F. Hilder, Charge heterogeneity profiling of monoclonal antibodies using low ionic strength ion-exchange chromatography and well-controlled pH gradients on monolithic columns, J. Chromatogr. A 1317 (2013) 148–154, https://doi.org/10.1016/j.chroma.2013.08.061.
[23] A.J. Link, Multidimensional peptide separations in proteomics, Trends Biotechnol. 20 (12) (2002), https://doi.org/10.1016/S1471-1931(02)00202-1 s8-s13.
[24] T. Ahamed, S. Chilamkurthi, B.K. Nfor, P.D.E.M. Verhaert, G.W.K. van Dedem, L.A. M. van der Wielen, M.H.M. Eppink, E.J.A.X. van de Sandt, M. Ottens, Selection of pH-related parameters in ion-exchange chromatography using pH-gradient operations, J. Chromatogr. A 1194 (1) (2008) 22–29, https://doi.org/10.1016/j.chroma.2007.11.111.
[25] N. Lingg, E. Tan, B. Hintersteiner, M. Bardor, A. Jungbauer, Highly linear pH gradients for analyzing monoclonal antibody charge heterogeneity in the alkaline range, J. Chromatogr. A 1319 (2013) 65–71, https://doi.org/10.1016/j.chroma.2013.10.028.
[26] G. Yang, L. Bai, C. Yan, Y. Gu, J. Ma, Preparation of a strong-cation exchange monolith by a novel method and its application in the separation of IgG on high performance liquid chromatography, Talanta 85 (5) (2011) 2666–2672, https://doi.org/10.1016/j.talanta.2011.08.048.
[27] K. Wrzosek, M. Polakovič, Effect of pH on protein adsorption capacity of strong cation exchangers with grafted layer, J. Chromatogr. A 1218 (39) (2011) 6987–6994, https://doi.org/10.1016/j.chroma.2011.07.097.
[28] X. Cui, W. Mi, Z. Hu, X. Li, B. Meng, X. Zhao, X. Qian, T. Zhu, W. Ying, Global characterization of modifications to the charge isomers of IgG antibody, J. Pharm. Anal. 12 (1) (2022) 156–163, https://doi.org/10.1016/j.jpha.2020.11.006.
[29] H. Lau, D. Pace, B. Yan, T. McGrath, S. Smallwood, K. Patel, J. Park, S.S. Park, R. F. Latypov, Investigation of degradation processes in IgG1 monoclonal antibodies by limited proteolysis coupled with weak cation-exchange HPLC, J. Chromatogr. B 878 (11) (2010) 868–876, https://doi.org/10.1016/j.jchromb.2010.02.003.
[30] K.J. Hassel, C. Moresoli, Role of pH and Ionic strength on weak cation exchange macroporous Hydrogel membranes and IgG capture, J. Membr. Sci. 498 (2016) 158–166, https://doi.org/10.1016/j.memsci.2015.08.058.
[31] H. Liu, W. Ren, L. Zong, J. Zhang, Y. Wang, Characterization of recombinant monoclonal antibody charge variants using WCX chromatography, icIEF and LC-MS/MS, Anal. Biochem. 564-565 (2019) 1–12, https://doi.org/10.1016/j.ab.2018.10.002.
[32] A. Beck, H. Diemer, D. Ayoub, F. Debaene, E. Wagner-Rousset, C. Carapito, A. Van Dorsselaer, S. Sanglier-Cianférani, Analytical characterization of biosimilar antibodies and Fc-fusion proteins, TrAC, Trends Anal. Chem. 48 (2013) 81–95, https://doi.org/10.1016/j.trac.2013.02.014.
[33] A. Murisier, E. Farsang, K. Horváth, M. Lauber, A. Beck, D. Guillarme, S. Fekete, Tuning selectivity in cation-exchange chromatography applied for monoclonal antibody separations, part 2: evaluation of recent stationary phases, J. Pharm. Biomed. Anal. 172 (2019) 320–328, https://doi.org/10.1016/j.jpba.2019.05.011.
[34] S.A. Berkowitz, J.R. Engen, J.R. Mazzeo, G.B. Jones, Analytical tools for characterizing biopharmaceuticals and the implications for biosimilars, Nat. Rev. Drug Discov. 11 (7) (2012) 527–540, https://doi.org/10.1038/nrd3746.
[35] S. Fekete, D. Guillarme, P. Sandra, K. Sandra, Chromatographic, electrophoretic, and mass spectrometric methods for the analytical characterization of protein biopharmaceuticals, J. Anal. Chem. 88 (1) (2016) 480–507, https://doi.org/10.1021/acs.analchem.5b04561.
[36] S. Hober, K. Nord, M. Linhult, Protein A chromatography for antibody purification, J. Chromatogr. B 848 (1) (2007) 40–47, https://doi.org/10.1016/j.jchromb.2006.09.030.
[37] H.G. Lee, S. Kang, J.S. Lee, Binding characteristics of staphylococcal protein A and streptococcal protein G for fragment crystallizable portion of human immunoglobulin G, Comput. Struct. Biotechnol. J. 19 (2021) 3372–3383, https://doi.org/10.1016/j.csbj.2021.05.048.
[38] L. Jendeberg, M. Tashiro, R. Tejero, B.A. Lyons, M. Uhlén, G.T. Montelione, B. Nilsson, The mechanism of binding staphylococcal protein A to immunoglobin G does not involve helix unwinding, Biochemistry 35 (1) (1996) 22–31, https://doi.org/10.1021/bi9512814.
[39] D. Shukla, L. Zamolo, C. Cavallotti, B.L. Trout, Understanding the role of arginine as an eluent in affinity chromatography via molecular computations, J. Phys. Chem. B 115 (11) (2011) 2645–2654, https://doi.org/10.1021/jp111156z.
[40] T. Arakawa, K. Tsumoto, K. Nagase, D. Ejima, The effects of arginine on protein binding and elution in hydrophobic interaction and ion-exchange chromatography, Protein Expr. Purif. 54 (1) (2007) 110–116, https://doi.org/10.1016/j.pep.2007.02.010.
[41] R. Sadighi, V. de Kleijne, S. Wouters, K. Lubbers, G.W. Somsen, A.F.G. Gargano, R. Haselberg, Online multimethod platform for comprehensive characterization of monoclonal antibodies in cell culture fluid from a single sample injection - Intact protein workflow, Anal. Chim. Acta 1287 (2024) 342074, https://doi.org/10.1016/j.aca.2023.342074.
[42] L. Verscheure, G. Vanhoenacker, S. Schneider, T. Merchiers, J. Storms, P. Sandra, F. Lynen, K. Sandra, 3D-LC-MS with 2D multimethod option for fully automated assessment of multiple attributes of monoclonal antibodies directly from cell culture supernatants, Anal. Chem. 94 (17) (2022) 6502–6511, https://doi.org/10.1021/acs.analchem.1c05461.
[43] S. Bhattacharya, S. Joshi, A.S. Rathore, A native multi-dimensional monitoring workflow for at-line characterization of mAb titer, size, charge, and glycoform heterogeneities in cell culture supernatant, J. Chromatogr. A 1696 (2023) 463983, https://doi.org/10.1016/j.chroma.2023.463983.
[44] W.L. DeLano, M.H. Ultsch, A.M. de Vos, J.A. Wells, Convergent solutions to binding at a protein-protein interface, Science 287 (5456) (2000) 1279–1283, https://doi.org/10.1126/science.287.5456.1279.
[45] J. Deisenhofer, Crystallographic refinement and atomic models of a human Fc fragment and its complex with fragment B of protein A from staphylococcus aureus at 2.9- and 2.8-.ANG. resolution, Biochemistry 20 (9) (1981) 2361–2370, https://doi.org/10.1021/bi00512a001.
[46] S. Kumar, T.S. Savane, A.S. Rathore, Multiattribute monitoring of aggregates and charge variants of monoclonal antibody through native 2D-SEC-MS-WCX-MS, J. Am. Soc. Mass Spectrom. (2023), https://doi.org/10.1021/jasms.2c00325.
[47] S. Jaag, M. Shirokikh, M. Lämmerhofer, Charge variant analysis of protein-based biopharmaceuticals using two-dimensional liquid chromatography hyphenated to mass spectrometry, J. Chromatogr. A 1636 (2021) 461786, https://doi.org/10.1016/j.chroma.2020.461786.
[48] G. Lambiase, S.E. Inman, M. Muroni, V. Lindo, M.J. Dickman, D.C. James, High-throughput multiplex analysis of mAb aggregates and charge variants by automated two-dimensional size exclusion-cation exchange chromatography coupled to mass spectrometry, J. Chromatogr. A 1670 (2022) 462944, https://doi.org/10.1016/j.chroma.2022.462944.
[49] T. Arakawa, J.S. Philo, K. Tsumoto, R. Yumioka, D. Ejima, Elution of antibodies from a Protein-A column by aqueous arginine solutions, Protein Expr. Purif. 36 (2) (2004) 244–248, https://doi.org/10.1016/j.pep.2004.04.009.
[50] L.T. Cordova, H. Dahodwala, K.S. Elliott, J. Baik, D.C. Odenewelder, D. Nmagu, B. A. Skelton, L. Uy, S.R. Klaubert, B.F. Synoground, D.G. Chitwood, V.G. Dhara, H. M. Naik, C.S. Morris, S. Yoon, M. Betenbaugh, J. Coffman, F. Swartzwelder, M. Gilmeister, S.W. Harcum, K.H. Lee, Generation of reference cell lines, media, and a process platform for CHO cell biomanufacturing, Biotechnol. Bioeng. 120 (3) (2023) 715–725, https://doi.org/10.1002/bit.28290.

[51] A. Technologies, Agilent Biocolumns Charge Variant Analysis Application Compendium, (2021).
[52] B. Sissolak, N. Lingg, W. Sommeregger, G. Striedner, K. Vorauer-Uhl, Impact of mammalian cell culture conditions on monoclonal antibody charge heterogeneity: an accessory monitoring tool for process development, J. Ind. Microbiol. Biotechnol. 46 (8) (2019) 1167–1178, https://doi.org/10.1007/s10295-019-02202-5.
[53] Z. Weng, J. Jin, C. Shao, H. Li, Reduction of charge variants by CHO cell culture process optimization, Cytotechnology 72 (2) (2020) 259–269, https://doi.org/10.1007/s10616-020-00375-x.
[54] Y. Du, A. Walsh, R. Ehrick, W. Xu, K. May, H. Liu, Chromatographic analysis of the acidic and basic species of recombinant monoclonal antibodies, MAbs 4 (5) (2012) 578–585, https://doi.org/10.4161/mabs.21328.
[55] Y. Leblanc, C. Ramon, N. Bihoreau, G. Chevreux, Charge variants characterization of a monoclonal antibody by ion exchange chromatography coupled on-line to native mass spectrometry: case study after a long-term storage at +5°C, J Chromatogr B Analyt Technol Biomed Life Sci 1048 (2017) 130–139, https://doi.org/10.1016/j.jchromb.2017.02.017.
[56] A.J. Schadock-Hewitt, R.K. Marcus, Initial evaluation of protein A modified capillary-channeled polymer fibers for the capture and recovery of immunoglobulin G, J Sep Sci 37 (5) (2014) 495–504, https://doi.org/10.1002/jssc.201301205.
[57] H.K. Trang, R.K. Marcus, Application of protein A-modified capillary-channeled polymer polypropylene fibers to the quantitation of IgG in complex matrices, J. Pharm. Biomed. Anal. 142 (2017) 49–58.
[58] S.K. Wysor, R.K. Marcus, Alleviation of the necessity for supernatant prefiltering in the protein a recovery of monoclonal antibodies from chinese hamster ovary cell cultures, J. Chromatogr. (2023). B in press.
[59] L. Jiang, R.K. Marcus, Microwave-assisted, grafting polymerization modification of Nylon 6 capillary-channeled polymer fibers for enhanced weak cation exchange protein separations, Anal. Chim. Acta 954 (2017) 129–139.